

EXPERIMENTAL REVIEW OF
BEAM POLARIZATION IN HIGH ENERGY e^+e^- STORAGE RINGS*

R. F. Schwitters
Stanford Linear Accelerator Center
Stanford University, Stanford, California 94305

I. INTRODUCTION

In 1964, Sokolov and Ternov¹ showed that under certain conditions, synchrotron radiation with spin-flip should lead to a gradual build-up of spin polarization of electrons and positrons circulating in a storage ring. This observation opened up the possibility of having practical sources of polarized e^+e^- beams which could be exploited for studying high energy physics.

In this paper, I review what information is provided by beam polarization in high energy e^+e^- interactions, how polarized beams are produced, the experimental evidence for radiative beam polarization, and the results which have been obtained to date using polarized beams. I conclude with a discussion of prospects for beam polarization experiments in future generations of storage rings.

II. POLARIZATION EFFECTS IN e^+e^- ANNIHILATION

One of the principal advantages of studying high energy phenomena with e^+e^- collisions is the simplicity of the e^+e^- initial state. At currently accessible energies ($E_{c.m.} \lesssim 25$ GeV), reactions involving annihilation of an electron and positron are mediated predominantly by the one-photon intermediate state. Thus, the net quantum numbers of the final state particles are the same as those of the photon, namely $J^{PC} = 1^{--}$, and only two helicity states, $\lambda = \pm 1$, are allowed.

As discussed below, synchrotron radiation involving spin-flip yields transversely polarized beams where the spins of the electrons, positrons are predominantly parallel, antiparallel to the guide magnetic field of the storage ring. If the beams are so polarized, the e^+e^- pair annihilate through a state having the properties of a linearly polarized photon, and the most general single particle inclusive angular distribution can be written as:²

$$\frac{d\sigma}{d\Omega} = \frac{1}{2} \left[(\sigma_t + \sigma_\ell) + (\sigma_t - \sigma_\ell) (\cos^2 \theta + P^2 \sin^2 \theta \cos 2\phi) \right] \quad (1)$$

where σ_t , σ_ℓ are non-negative functions of particle type, particle energy, and center-of-mass energy; P is the degree of transverse

*Work supported by the Department of Energy under contract no. EY-76-C-03-0515.

(Invited talk presented at the III International Symposium on High Energy Physics with Polarized Beams and Polarized Targets, Argonne, Illinois, October 25-28, 1978.)

polarization of the beams (assumed to be equal in magnitude and opposite in direction for the two beams); θ , ϕ are the polar and azimuthal angles of the produced particle, as defined in Fig. 1.

The quantity of interest that can be determined by measurements of angular distributions is

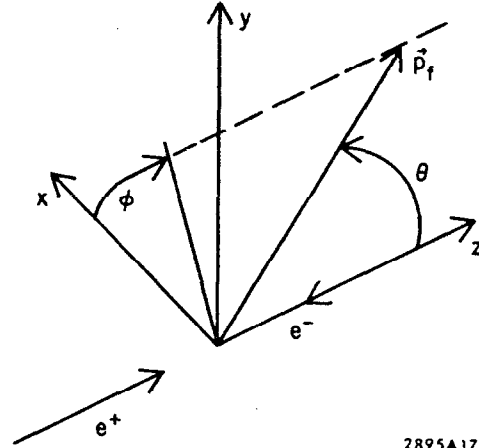
$$\alpha = \frac{\sigma_t - \sigma_\ell}{\sigma_t + \sigma_\ell};$$

it gives information on the production dynamics of the particle being studied. For example, $\alpha = +1$ in the case of pair production of spin- $\frac{1}{2}$ particles such as muons, while $\alpha = -1$ for pair production of pseudoscalars, such as pions. In multihadron production, α is bounded between these two extreme values and will, in general, depend on particle type, momentum, and center-of-mass energy.

It is evident from Eq. (1) that transverse beam polarization does not provide any new information that could not be determined by measurement of the polar angle dependence above. However, the azimuthal angle variation of inclusive cross sections is often technically easier to measure than the $\cos^2 \theta$ dependence because of the geometry of most detectors. This is because most detectors are nearly cylindrically symmetric with respect to the incident e^+e^- direction and have essentially full acceptance in azimuthal angle. Most detectors have less than complete acceptance in polar angle with losses occurring at large values of $\cos^2 \theta$. Thus, transversely polarized beams provide a convenient, if not necessary, means for determining the parameter in processes dominated by the one-photon exchange approximation. The combined θ - ϕ information with polarized beams allows a check of this approximation.

At the next generation of e^+e^- storage rings ($E_{c.m.} \gtrsim 30$ GeV), weak neutral current effects are expected to begin to play a significant role in e^+e^- annihilation. Various parity-violating phenomena could occur and some of these may be observed using longitudinally polarized beams. In what follows, the weak neutral current for spin- $\frac{1}{2}$ particles is assumed to be a mixture of vector and axial-vector parts. The interference between the electromagnetic current and the weak neutral current leads to the following e^+e^- spin dependence of the cross section for producing spin- $\frac{1}{2}$, point-like fermion pairs $f\bar{f}$:³

$$\sigma_f(\lambda_+, \lambda_-) = [(1 - \lambda_+ \lambda_-) + (\lambda_- - \lambda_+) H_f] \sigma_f(0, 0) \quad (2)$$



2895A17

Fig. 1. Coordinate system and definition of angles.

where λ_+ , λ_- are the longitudinal polarization of the incident e^+ , e^- beams, measured with respect to their directions of motion. The "low" energy behavior of H_f and $\sigma_f(0,0)$ can be described by:

$$\sigma_f(0,0) \approx \frac{4\pi}{3} \frac{\alpha^2}{s} Q_f^2 \quad (3)$$

$$H_f \approx \frac{-G s}{\sqrt{2} 4\pi\alpha} \frac{g_A^e g_V^f}{Q_f}$$

where α is the fine structure constant, G is the Fermi constant, s is the square of the center-of-mass energy, Q_f is the electric charge of particle f measured in units of the charge on the positron g_A^e is the weak axial vector coupling constant of the electron, and g_V^f is the weak vector coupling constant of the final state fermion f . At $E_{c.m.} = 30$ GeV, the quantity $Gs/\sqrt{2} 4\pi\alpha$ is approximately 0.081.

From Eqs. (2) and (3), it is seen that longitudinally polarized beams would provide new information, namely a measurement of the coupling constant g_V^f (assuming g_A^e is known from other measurements). (It is possible to determine the weak axial-vector coupling constant of f , g_A^f , by measuring the front-back angular asymmetry in the production of $f\bar{f}$ pairs.) It is interesting to note that if the incident beams are fully longitudinally polarized in opposite directions, the total annihilation production rate will vanish!

III. RADIATIVE BEAM POLARIZATION

All experimental work performed to date with polarization in high energy e^+e^- storage rings has relied on the fact that under certain conditions, the beams become transversely polarized through the mechanism of synchrotron radiation with spin-flip. This is called radiative beam polarization and was first discussed by Ternov, Lokutov, and Korovina in 1961.⁴ In 1963, Sokolov and Ternov¹ showed that the transverse polarization for particles circulating in a uniform magnetic field would build up in time according to:

$$P(t) = \frac{8\sqrt{3}}{15} \left(1 - e^{-t/T_{pol}} \right) \quad (5)$$

$$\frac{1}{T_{pol}} = \frac{5\sqrt{3}}{8} \frac{e^2 \hbar \gamma^5}{m c^2 \rho^3}$$

where γ is the Lorentz factor of the particle ($\equiv E/m$) and ρ is the bending radius of the orbit. Positrons, electrons would become polarized parallel, antiparallel to the magnetic field. Baier and Katkov,⁵ in 1967, generalized this result to include inhomogeneous magnetic fields and obtained the following general expression for the

transition probability per unit time for spin flip:

$$W^{\uparrow\downarrow} = \frac{5\sqrt{3}}{16} \frac{e^2 \hbar}{m^2 c^5} \gamma^5 |\vec{\beta}|^3 \left[1 - \frac{2}{9} (\vec{S} \cdot \hat{\beta})^2 + \frac{8\sqrt{3}}{15} \vec{S} \cdot (\hat{\beta} \times \dot{\hat{\beta}}) \right] \quad (5)$$

where \vec{S} is the initial spin direction in the electron rest frame, $\hat{\beta}$ and $\dot{\hat{\beta}}$ are unit vectors in the velocity, acceleration directions, respectively, and $\vec{\beta}$ is the acceleration, measured in the laboratory frame. A complete discussion of this phenomenon is presented in the review article by Baier⁶ and a detailed pedagogical derivation of Eq. (5) is given in the review article by Jackson.⁷

When combined with the usual Thomas-BMT equation of spin motion,⁸ Eq. (5) leads to damping terms that give rise to a build-up of polarization described in Eq. (4), in the case of a conventional separated function storage ring. When the guide bending magnets all have the same value of magnetic field, the time constant for polarization build-up is

$$T_{\text{pol}}(\text{sec}) = \frac{98.7 \times |\rho(\text{m})|^3}{|E(\text{GeV})|^5} \times \frac{R}{\rho} \quad (6)$$

where E is the beam energy in GeV, ρ is the bending radius in units of meters and R is the average radius of the storage ring. The most distinctive feature of Eq. (6) is the very strong energy dependence. For example, the SPEAR storage ring, operating at 3.7 GeV per beam, has a build-up time of approximately 14 minutes.

A necessary condition for radiative polarization to occur is that spin motion along the polarization direction be stable over time scales on the order of or greater than T_{pol} . The Novosibirsk group has made the major contributions to the study of the stability of spin motion in e^+e^- storage rings. The classic papers of Derbenev and Kondratenko^{9,10} contain the general results; the review papers of Baier⁶ and Derbenev, Kondratenko, and Skrinsky¹¹ are useful references on depolarization phenomena. The basic result of this work is that there exist depolarization mechanisms in conventional storage rings that will lead to a reduction in the asymptotic polarization P_{max} from 92.4% to:

$$P_{\text{max}} = \frac{8\sqrt{3}}{15} \times \frac{1}{1 + \frac{T_{\text{pol}}}{T_{\text{depol}}}} \quad (7)$$

where T_{depol} is the characteristic time for depolarization. (The results on depolarization presented in Refs. 9 and 10 are not restricted to the simple storage ring geometry considered here.)

Briefly, spin motion in a conventional storage ring is simply Thomas-Larmor precession about the vertical direction. The spin

precession frequency ν represents the number of precessions in advance of the orbital motion that the spin experiences during each orbital period; it is given by

$$\nu = \gamma \frac{(g-2)}{2} \approx \frac{E(\text{GeV})}{0.44065} \quad (8)$$

where g is the gyromagnetic ratio of the electron.

In addition to the main bending field, the particles exhibit betatron and synchrotron motion and experience various focusing and acceleration fields. These also affect the spin motion. The electromagnetic fields set up by the opposing beam are a further strong perturbation to both orbital and spin motion. These three general mechanisms that can lead to depolarization may be summarized by:

1. Resonance depolarization
2. Stochastic depolarization
3. Beam-beam effects.

Resonance depolarization occurs when the spin precession frequency is integrally related to characteristic frequencies of orbital motion according to:

$$\nu = n \pm i\nu_x \pm j\nu_y \pm k\nu_s \quad (9)$$

where n, i, j, k are integers, ν_x and ν_y are the horizontal and vertical betatron tunes, and ν_s is the synchrotron frequency. The most prominent depolarization resonances are usually the integer resonances, $\nu=n$, and the first order sidebands where i or j equals 1. The integer resonances repeat every 440 MeV in beam energy.

Stochastic depolarization arises primarily from the transverse focusing fields experienced by a particle during cycles consisting of the emission of synchrotron radiation followed by the build-up and damping of betatron and synchrotron motion. This gives rise to depolarization away from the important resonances. Stochastic depolarization rates are sensitive to beam sizes and orbit distortions. There now exist standard computer codes¹² for calculating resonance and stochastic depolarization effects.

The beam-beam interaction exerts strong, non-linear forces on the particles and is expected to play a role in depolarization through its effect on orbital motion as well as its direct influence on spin. Currently, beam-beam forces are poorly understood and their effect on polarization cannot be computed with reliability. A discussion of beam-beam interaction effects on polarization is contained in Ref. 11.

The first experimental indications of radiative polarization were obtained in the late 1960's and 1970 at Orsay and Novosibirsk. Unambiguous evidence for the radiative build-up of polarization was reported in 1971 by both the Novosibirsk group⁶ and the Orsay group¹³

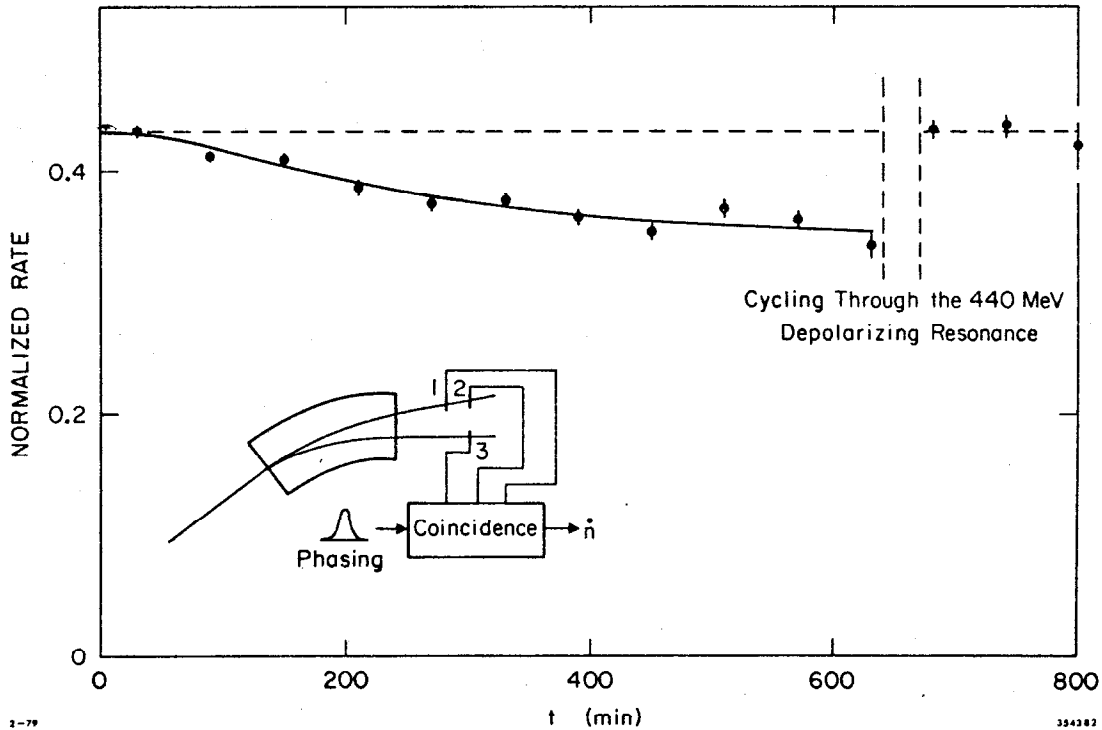


Fig. 2. Schematic diagram of Touschek scattering setup and experimental results of the Orsay group.¹³ The data show the reduction in Touschek rate caused by the build-up of transverse polarization. Near the end of the data run, the beam was depolarized by changing beam energy through a spin resonance.

using the storage ring ACO. The Orsay group, in 1973, reported¹⁴ on more detailed measurements performed at ACO. They found evidence for betatron-frequency-sideband depolarizing resonances and showed that polarization persists in the presence of colliding beams. One particularly interesting measurement made during this study was the polarization of one beam as a function of the current of the other colliding beam when the beam energy was fixed near the vertical betatron sideband resonance. At high currents, the polarization was large, at somewhat lower current it was reduced, and at still lower current, it became large again. This is interpreted as evidence for the linear betatron tune shift of one beam caused by focusing forces that are proportional to the intensity of the oncoming beam. At one value of current, the tune shift was the value necessary to satisfy the spin resonance condition and the beam depolarized. At higher or lower currents the tune shift was either too large or too small to satisfy the resonance condition. This is a good example of the accelerator diagnostic possibilities of polarized beams. In a completely non-perturbative way, spin frequency information can be used to probe betatron motion where conventional techniques may not be possible.

In 1975, the observation of radiative beam polarization of the expected level and build-up rate was reported from SPEAR.¹⁵ At about this time, as will be discussed later, experiments making use of polarized beams began at Novosibirsk and at SPEAR.

In all of these early observations of radiative polarization, the one basic technique employed for measuring polarization was the measurement of the Touschek scattering rate. The details of the method can be found in the review article of Baier⁶ and in a paper by Ford, Mann, and Ling.¹⁶ Briefly, Touschek scattering is Møller scattering of electrons or positrons within a single rf bucket. When viewed from a reference frame moving with a bunch of electrons, the individual particles have typical momenta on the order of a few hundred keV and they scatter with other particles in the bunch. The scattering rate will depend on polarization. If two particles, which were originally moving toward each other in a direction perpendicular to the bunch velocity direction, scatter at a large angle such that they travel nearly parallel to the bunch direction after scattering then their Lorentz transformed laboratory energies will be significantly different after the scattering occurred and the particles may be lost from the beam. This can be an important loss mechanism in e^+e^- storage rings. By measuring the rate for the correlated loss of pairs of particles from a single beam, one has a measure of the intra-beam Møller scattering which, in turn, depends on polarization. A typical experimental set-up and series of measurements is shown in Fig. 2.

The experiments performed at Novosibirsk and Orsay demonstrated the essential features of radiative beam polarization. First, the beams do indeed become transversely polarized with the time dependence given by Eq. (4). This can be seen quite well from the nice results of the Novosibirsk group¹⁷ shown in Fig. 3. As previously mentioned, depolarizing effects can be important and their expected behavior seems to be born out by the Novosibirsk and Orsay experiments.

In order to perform more detailed measurements of depolarizing phenomena, our group¹⁸ has recently developed a back-scattered laser polarimeter. As first pointed out by Baier and Khoze,¹⁹ Compton scattering of circularly polarized optical photons by a high energy transversely polarized beam is a sensitive and direct method for

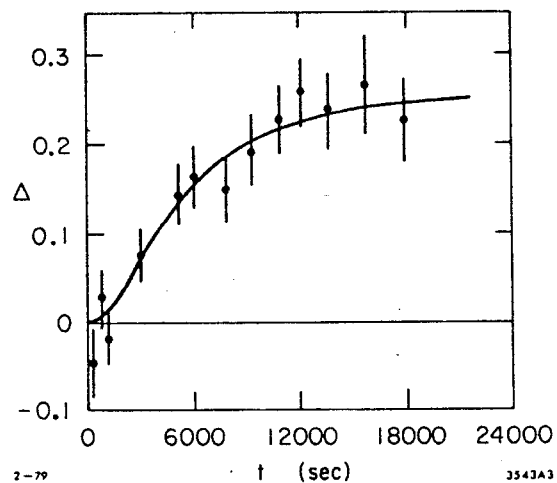


Fig. 3. Polarization build-up observed by Novosibirsk group¹⁷ with Touschek scattering method. Build-up rate agrees with Eq. (4).

measuring the beam polarization. We chose this method rather than Touschek scattering for several reasons. First, the analyzing power and counting rate for a laser system can be accurately calculated, while the Touschek rate depends sensitively on the beam size and intensity, introducing uncertainty in the analyzing power. Many possible systematic errors can be checked by varying the polarization of the laser beam; such systematic checks are not available in the Touschek method. At high energies, Touschek scattering losses represent a relatively small fraction of the total particle loss rate. Thus, backgrounds became very important, whereas the backgrounds in the laser case can be made quite small and can be accurately measured by simply turning off the laser. The goal of our development project was to design a monitor that could make polarization measurements to the 10% level of accuracy in one or two minutes and to study depolarization effects with this device.

The experimental set-up is shown schematically in Fig. 4. An Argon-ion laser supplies the photons which are alternately switched between right and left circular polarization at a rate of approximately 25 Hz by means of an electro-optic device known as a Pockel's cell. The laser is operated in a cavity-dumped mode so that the beam of circularly polarized photons can be pulsed in synchronism with the 1.28 MHz resolution frequency of the single e^+ bunch normally stored in SPEAR. The peak laser intensity is approximately 80 watts; the photon energy is about 2.4 eV (green in color). The backscattered gamma rays are contained in a cone of characteristic angle $1/\gamma$ where γ is the Lorentz factor of the e^+ and the maximum gamma-ray energy is of order 100 MeV depending on e^+ energy. The light beam crosses the e^+ beam vertically at an angle of 8 mr; the intersection point was chosen so that the e^+ beam converged in the vertical direction causing the backscattered gamma rays to be focused vertically at a point approximately 13 meters from the intersection point. Here was placed a gamma-ray detector that could accurately measure the vertical distribution of the backscattered gamma rays. We have used two detectors: One, a multiwire proportional chamber with 1 mm wire spacing and a gamma-ray converter, was used for most of the data presented here. The second, consisting of a converter and single cell drift chamber with approximately 0.2 mm resolution vertically, is currently being used. Both detectors have performed satisfactorily.

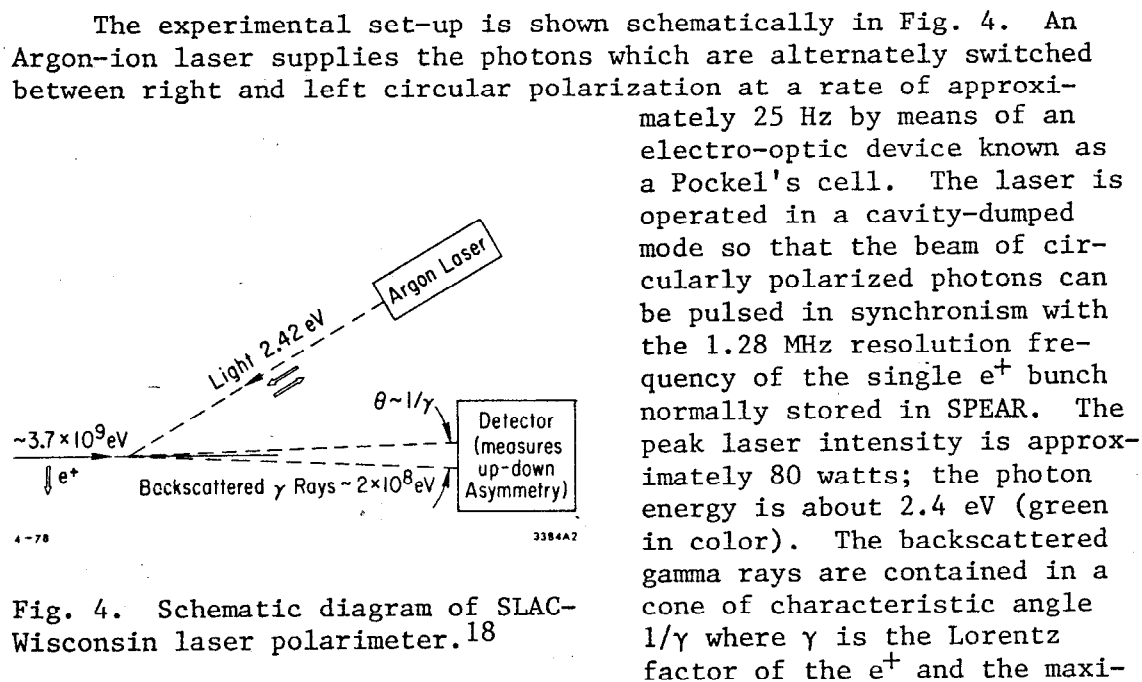


Fig. 4. Schematic diagram of SLAC-Wisconsin laser polarimeter.¹⁸

The light beam crosses the e^+ beam vertically at an angle of 8 mr; the intersection point was chosen so that the e^+ beam converged in the vertical direction causing the backscattered gamma rays to be focused vertically at a point approximately 13 meters from the intersection point. Here was placed a gamma-ray detector that could accurately measure the vertical distribution of the backscattered gamma rays. We have used two detectors: One, a multiwire proportional chamber with 1 mm wire spacing and a gamma-ray converter, was used for most of the data presented here. The second, consisting of a converter and single cell drift chamber with approximately 0.2 mm resolution vertically, is currently being used. Both detectors have performed satisfactorily.

The basic measurement being made is an up-down asymmetry in the yield of backscattered gamma rays that is proportional to the transverse beam polarization. This asymmetry changes sign when the helicity of the incident photon beam is reversed. Thus, to minimize systematic errors, we rapidly alternate between right and left circular polarization of the laser beam and compute the average asymmetry, taking into account the change in sign, for the two helicities. A microcomputer system tallies asymmetries, gates the laser on and off for determining background, times the experimental runs, and prints out results. The analyzing power for the system is approximately 2.5% and a typical counting rate is 10 kHz; the usual data run requires two minutes and yields a value for the average up-down asymmetry accurate to $\pm 0.1\%$.

Figure 5 shows the up-down asymmetry as a function of time for a beam energy of 3.7 GeV. The data are in excellent agreement with expected polarization build-up rate.

The first set of detailed measurements that we have made was to study the ratio of depolarization rate to build-up rate as a function of beam energy for single e^+ beams. This ratio is extracted from the polarization build-up time constant, without resort to using absolute asymmetry, according to:

$$\frac{1}{T_{\text{obs}}} = \frac{1}{T_{\text{pol}}} \left(1 + \frac{T_{\text{pol}}}{T_{\text{depol}}} \right) \quad (10)$$

$$A_{\text{obs}}(t) = A \left(1 - e^{-t/T_{\text{obs}}} \right)$$

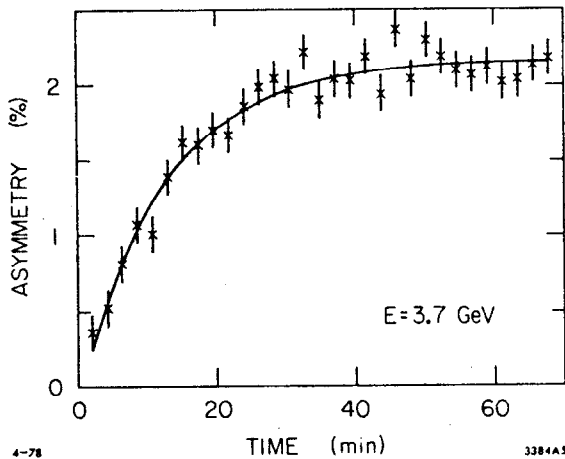


Fig. 5. Polarization build-up measured at SPEAR.¹⁸ Solid line is a fit to the data using Eq. (10). At this energy, depolarization is negligible.

where T_{obs} is the observed time constant for the measured asymmetry A_{obs} , which can be determined without independently knowing the value A . In such measurement, the polarization is allowed to reach nearly its asymptotic value, then the beam energy is changed by a few MeV and a new asymmetry is reached. This process is repeated several times until a given sweep in energy is completed, or the positron intensity drops to an unacceptably low level. The data from a typical scan are presented in Fig. 6. The curve is a fit to the data assuming a constant analyzing power and that the polarization at the beginning of each new energy point equals the

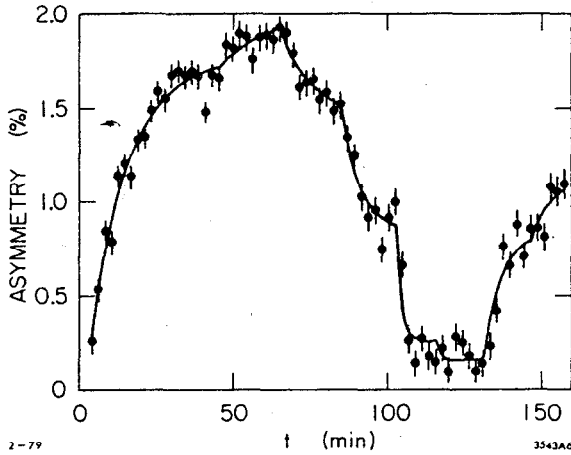


Fig. 6. Polarization scan measured at SPEAR.¹⁸ Breaks in solid line indicate times where the beam energy was changed. The line is a fit to the data using Eq. (10), but with different depolarization rates for each energy setting.

polarization at the end of the previous energy setting. Breaks in the solid curve indicate new energy settings. The data show the usual build-up, then as the energy or spin frequency approaches a resonant value, the asymmetry quickly drops according to Eqs. (9) and (10), until it essentially vanishes. At slightly higher energies, the asymmetry re-emerges. The fitted values for the ratio of depolarization rate to build-up rate are given in Fig. 7 along with a theoretical calculation.¹² The theory and data are in excellent agreement and clearly show the presence of a strong spin resonance at a sideband due to horizontal betatron motion and a weaker resonance corresponding to the vertical betatron tune.

These measurements will continue with single beams and colliding beams with the goals of thoroughly checking the single beam theory and attempting to learn more about the beam-beam interaction. From the measurements we have already made, we can make the following preliminary conclusions:

1. The theoretical descriptions of the radiative build-up of transverse polarization and depolarization due to resonant and stochastic effects in single beams appear to be accurate. Depolarization resulting from forces that are non-linear in excursions of the particle motion from the equilibrium orbit appears to be rather weak.
2. A high degree of polarization can exist when the beams are colliding. However, various non-reproducible effects were observed indicating the need for much more study in this area.

IV. EXPERIMENTS WITH POLARIZED BEAMS

The natural, transverse polarization acquired by stored beams of high energy electrons and positrons have been put to use in a number of experiments. These experiments fit into two general categories, those where the Thomas-Larmor precession of the e^+ or e^- is exploited, and those where angular distributions of final state particles from e^+e^- annihilation are measured.

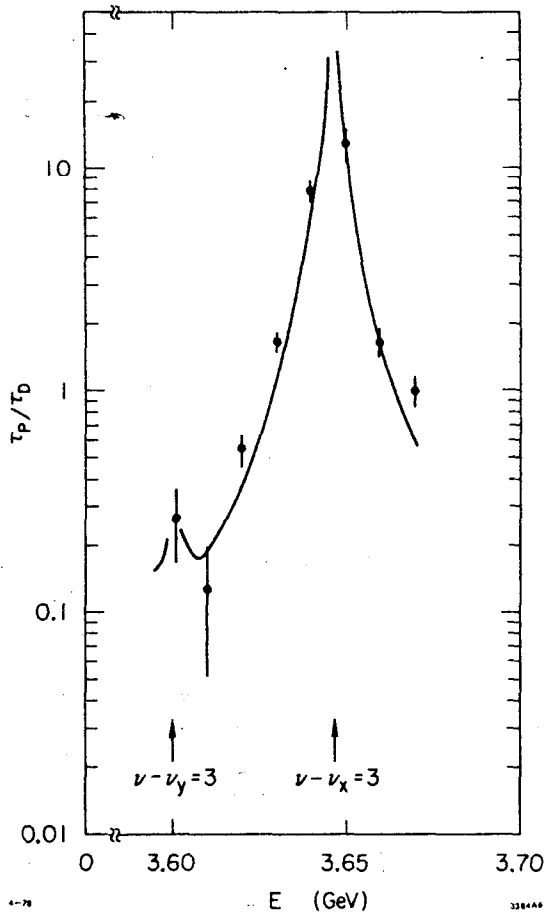


Fig. 7. Ratio of depolarization rate to polarization rate as a function of beam energy derived from the data shown in the previous figure. Positions of the two important betatron sideband spin resonances in this energy range are indicated.

ference between the anomalous magnetic moments ($a = (g-2)/2$) of electrons and positrons:

$$|a_{e^+} - a_{e^-}| < 1.0 \times 10^{-5} \quad (95\% \text{ confidence level}) \quad .$$

This is about two orders of magnitude more sensitive than previous measurements, which involved direct measurements of a_{e^+} and a_{e^-} in different experiments.

The resonant depolarization technique developed at Novosibirsk,¹⁷ combined with the very accurately known value of a_e^- (Ref. 21) provide a precise tool for calibrating the energy of e^+e^- storage rings. This has been done for VEPP-2M (Ref. 22) and yielded the following

The Novosibirsk group has reported results in both categories. S. I. Serednyokov *et al.*²⁰ performed a high precision comparison of the anomalous magnetic moments of the electron and positron in an experiment using the VEPP-2M storage ring. Their basic measurement was a comparison of the spin precession frequencies ν^+ , ν^- of e^+ , e^- beams simultaneously stored. The beams were allowed to polarize for two characteristic time intervals ($T_{\text{pol}} \approx 1$ hr, $E = 625$ Mev). Then an oscillating longitudinal magnetic field was applied to the beams and the driving frequency f_D of this field was slowly swept. The polarization was monitored by two identical Touschek scattering detectors, one for each of the e^+ and e^- beams. When the resonance condition

$$f_D^\pm = \frac{\Omega_0}{2\pi} (\nu^\pm - 1) \quad (11)$$

is met (Ω_0 is the revolution frequency), the e^+ beam depolarizes rapidly and will give a jump in the corresponding Touschek scattering rate at that frequency. The group found that $|f_D^+ - f_D^-| < 250$ Hz which, according to Eq. (8), provides the following limit on the dif-

value for the ϕ , meson mass, which is produced directly as a resonance in e^+e^- annihilation:

$$M_\phi = 1019.48 \pm 0.13 \text{ MeV}/c^2.$$

The accurate energy calibration of VEPP-2M and a measurement of the kinetic energy of K^\pm mesons using nuclear emulsion, allowed the Novosibirsk group²³ to determine the charged kaon mass to

$$M_{K^\pm} = 493.670 \pm 0.029 \text{ MeV}.$$

Observations of effects due to transverse beam polarization on angular distributions of particles produced by e^+e^- annihilation were first reported in 1975. The electrodynamic reactions $e^+e^- \rightarrow e^+e^-$ (Bhabha scattering) and $e^+e^- \rightarrow \mu^+\mu^-$ were studied at SPEAR with the SLAC/LBL magnetic detector. Learned, Resvanis, and Spencer²⁴ analyzed the results of these measurements and found significant azimuthal variation in both reactions at the center-of-mass energy $E_{c.m.} = 2E_B = 7.4 \text{ GeV}$ that was consistent with the theory of quantum electrodynamics and indicated that the beams were polarized within 80% of the expected maximum value. Their results are presented in Fig. 8. At $E_B = 1.55 \text{ GeV}$, the beams are expected to be unpolarized, while at $E_B = 3.7 \text{ GeV}$, large azimuthal variations are seen in both reactions. Muon pair production has the angular distribution of Eq. (1) with $\sigma_\ell = 0$. Bhabha scattering has a more complicated angular distribution² because it does not proceed entirely by single photon annihilation. Kurdadze *et al.*²⁵ have also reported observation of the azimuthal variation in muon pair production at VEPP-2M.

The single-photon exchange picture of hadron production by e^+e^- annihilation has been confirmed through polarization studies. The Novosibirsk group²² measured the azimuthal variation of K meson pair production at the ϕ resonance and it is described by Eq. (1) with $\sigma_t = 0$, as expected.

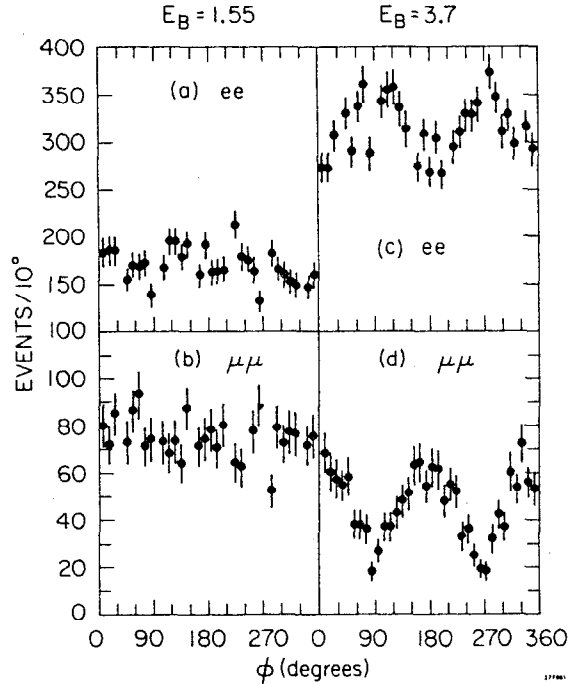


Fig. 8. Azimuthal angle distributions for muon pair production ($\mu\mu$) and Bhabha scattering (ee) measured at SPEAR²⁴ at two beam energies. At $E_B = 1.55 \text{ GeV}$ the beams were unpolarized; at $E_B = 3.7 \text{ GeV}$, they were over 70% polarized.

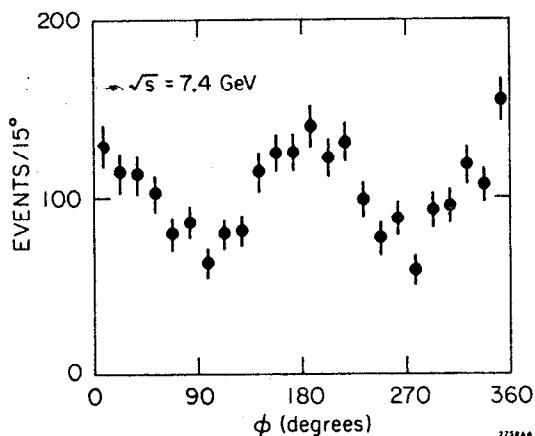


Fig. 9. Inclusive azimuthal angle distribution for hadrons with $x > 0.3$ measured at SPEAR.²⁶

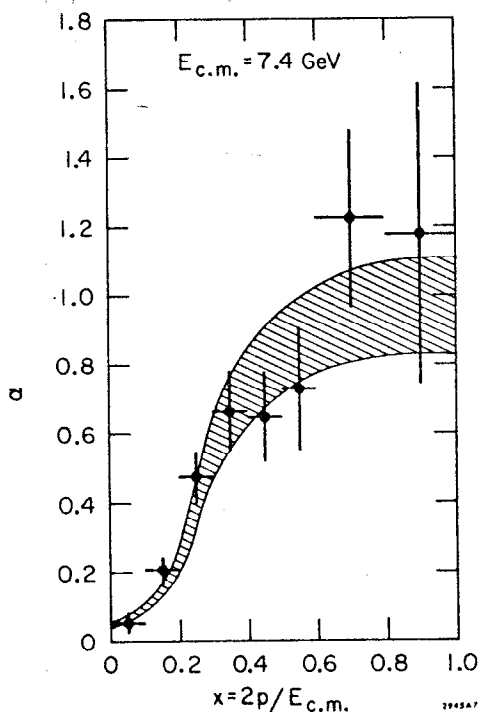


Fig. 10. The parameter α versus x for inclusive hadron production. The dashed region is the prediction of a jet model calculation.²⁷

Studies of multihadron production with polarized beams at the center-of-mass energy 7.4 GeV have been made by the SLAC/LBL collaboration at SPEAR.²⁶ All events having three or more charged hadrons within the angular region $|\cos \theta| \leq 0.7$ were selected. The average beam polarization was about 70%. Figure 9 shows the inclusive azimuthal angular distribution for all prongs in this event sample having $x > 0.3$ where x is the scaling variable, $x = 2p/E_{c.m.}$, and p is the particle momentum. The strong ϕ dependence is evident. The combined θ, ϕ distributions were fitted to Eq. (1) and values of the parameter α were obtained as a function of the scaling variable x . These are shown in Fig. 10. At small values of x , α approaches zero, while at large values, it approaches unity. Most of the hadrons in these events are pions, so it is significant that at large x they display the value of α corresponding to pair production of spin- $\frac{1}{2}$ particles rather than the value $\alpha = -1$ expected for meson pair production and observed in K^+K^- production at the ϕ mass. However, this is consistent with the quark-parton model where hadrons are created through the pair production of spin- $\frac{1}{2}$ quarks followed by their subsequent decay to ordinary hadrons. In this picture, the hadrons of higher momentum more closely follow the initial quark direction and retain the quark value of α , namely $\alpha = +1$.

This view is strengthened by the observation of jets in these same data.²⁷ Jets are multiparticle correlations where hadronic events display a preferred axis where components of momentum

perpendicular to this axis are limited to small values, the mean value of which is more or less independent of center-of-mass energy. Momenta parallel to the preferred or jet axis grow essentially linearly with increasing center-of-mass energy. Jets are exactly the kind of multiparticle correlations expected in the quark-parton model, where the direction of motion of the initial quark pair is the jet axis, and the fragmentation of the quarks into hadrons takes place along this axis with relatively small p_t . The polarized beam data show that the angular distribution of the jet axis corresponds to $\alpha_{jet} = 0.97 \pm 0.14$, in agreement with unity, the value expected for spin- $\frac{1}{2}$ quarks. The shaded region of Fig. 10 shows values of α vs. x one would expect for hadrons produced by fragmentation of quark pairs; the jet model calculations are in good agreement with these data.

To summarize, from experimental work performed to date, beam polarization has been shown to be a convenient energy calibration tool, the one-photon exchange approximation has been shown to be valid for electrodynamic and hadronic processes, and multihadron production fits well the simple spin- $\frac{1}{2}$ quark picture.

V. FUTURE PROSPECTS

We can expect polarized beams to continue to play an important role in future generations of e^+e^- colliding beam machines. In the present generation, PETRA and PEP, conventional radiative polarization should occur and it will provide convenient tools for precision energy calibration, non-destructive beam diagnostics, and probing one-photon exchange processes through the measurement of azimuthal asymmetries. Chao²⁸ has calculated the expected depolarization forces for PEP; these results are summarized in Fig. 11, where the asymptotic polarization is shown as a function of the beam energy. The polarization build-up time constant for PEP is about 20 minutes for a beam energy of 15 GeV. This relatively long time constant and the strong depolarizing resonances shown in Fig. 11 imply that practical experiments using radiative polarization may be limited to relatively narrow bands of energies at the high energy end of the PEP and PETRA energy ranges.

As we go to e^+e^- storage rings of even higher energy, these two effects combine to make it more difficult to use the natural radiative polarization. As discussed above, T_{pol} scales as $R^3 E^{-5}$. To optimize costs and performance for high energy storage rings,²⁹ it is necessary to increase the radius with energy according to:

$$R \propto E_{max}^p$$

where p lies between 2 and 3 for current technology. Therefore we can expect $T_{pol} \propto E_{max}^\epsilon$ where $1 \lesssim \epsilon \lesssim 4$. Thus, if nothing is done to control the polarization build-up rate, build-up times will become impractically long. The second deleterious effect present in storage

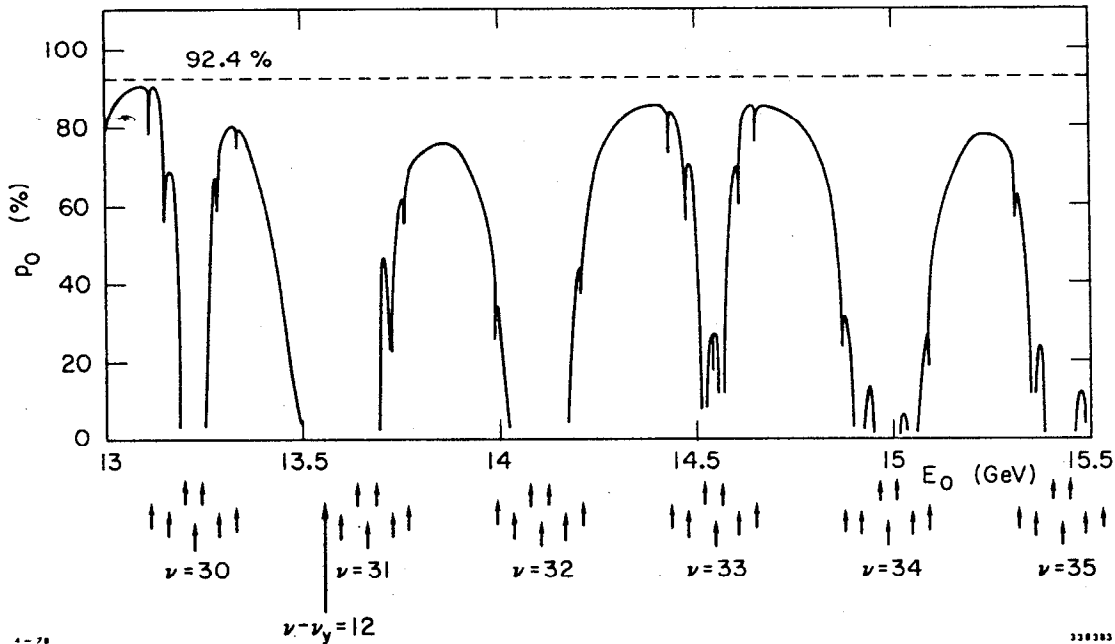


Fig. 11. Maximum transverse beam polarization expected at PEP.28

rings of higher energy is evident in Fig. 11. Depolarization resonances are spaced in bands every 440 MeV in beam energy and, therefore, these bands become relatively more dense as the energy is raised. Möhl and Montague³⁰ have estimated that at very high energies, above 100 GeV, the overlap of these resonance may overwhelm radiative build-up of polarization in conventional storage rings.

There appears to be at least a partial solution to the problem of prohibitively long time constants. Several workers³¹ have suggested using "wiggler" magnets to increase the polarization rate. These are reversed guide magnets that increase the total synchrotron radiation emitted on each revolution. Since T_{pol} is related to the strength B of the guide field by:

$$\frac{1}{T_{pol}} \propto \oint |B|^3 ds$$

where the integral is over a complete revolution, it is reduced by the addition of wiggler magnets. However, one must take care not to reduce the asymptotic polarization which is related to B by:

$$p_{max} = 92.4\% \times \frac{\oint B^3 ds}{\oint |B|^3 ds} .$$

The reverse wiggler magnets should be as weak as possible, while those having the same field direction as the guide field should be as strong as possible.

Looking further ahead, it would be extremely desirable to have longitudinally polarized beams. As mentioned in the introduction, such beams could be used to measure the weak vector coupling constants of quarks and leptons. At energies above the threshold for pair production of charged W bosons, longitudinal polarization would provide a detailed test of the interplay of the various subprocesses involved in W^+W^- pair production that are required by gauge theories in order to obtain finite cross sections.³²

If longitudinally polarized particles were injected into a conventional storage ring, they would quickly depolarize unless special care is taken with the guide magnetic field.³³ The basic strategy for overcoming this depolarization relies on the well known fact (Refs. 6, 9, and 10) that at every point on the closed orbit of a storage ring composed of essentially arbitrary static electric and magnetic fields, one can define a polarization direction about which the spin of an electron precesses by a constant phase advance on successive revolutions about the storage ring. Particles initially polarized along this direction will remain polarized unless subjected to the depolarization forces discussed previously. In a conventional storage ring, the polarization direction coincides with the guide field direction. However, by suitable choice of magnetic elements, it is possible to arrange the polarization direction to be parallel to the beam direction at certain positions on the equilibrium orbit, in particular, at intersection regions.

Two basic schemes have been devised for doing this.. In one method, a special set of magnets is inserted adjacent to an intersection region. These magnets are arranged to rotate the spin from the transverse direction to longitudinal at the interaction point, then rotate it back to transverse before re-entering the normal lattice of the storage ring. In this way, normal radiative build-up of polarization can take place in the regular guide magnets and no additional source of polarized particles is needed. Many specific magnet arrangements have been proposed for this transformation;^{11,31,33,34}

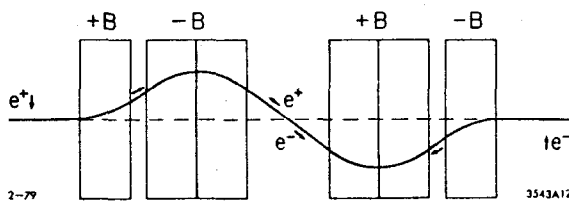


Fig. 12. Schematic diagram of one scheme for producing collisions of longitudinally polarized beams using the natural build-up of transverse polarization. Arrows indicate polarization directions. Boxes represent vertical bending magnets with horizontal fields $\pm B$.

a simple illustrative example is shown in Fig. 12. Here, a series of six vertical bending magnets, each having a bending power of approximately 2.3 t-m, will transform transverse spins to longitudinal and vice versa for electrons and positrons of all momenta. Chao²⁸ has calculated the maximum polarization that could be expected at PEP if such a scheme were employed; his results are plotted in Fig. 13. Beyond the obvious technical difficulties with these special spin rotating insertions, they

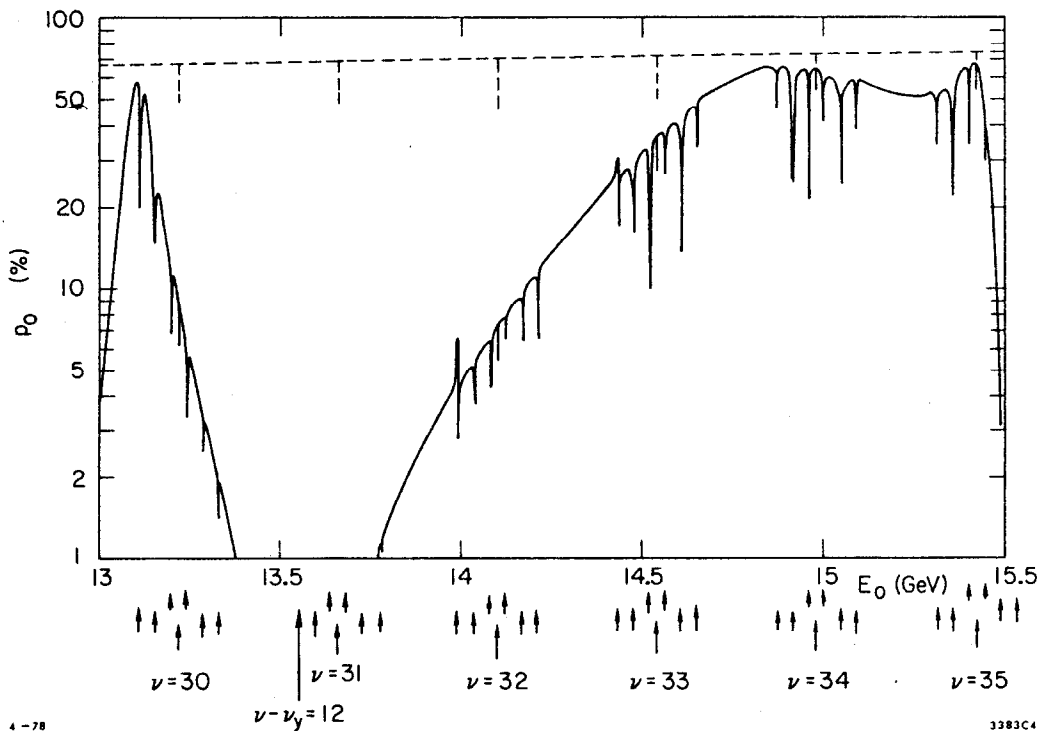


Fig. 13. Maximum longitudinal beam polarization expected at PEP²⁸ with a magnet system like the one shown in Fig. 12.

have the curious property that the electrons and positrons will have antiparallel spins. Therefore, if we are to avoid having the annihilation cross section vanish, it will be necessary to depolarize selectively one of the beams.

The second general scheme for providing longitudinally polarized beams has been christened the Siberian Snake in honor of its development at Novosibirsk through the work of Derbenev and Kondratenko³⁵ and others. Here one plays a topological trick on the spin motion. By placing a solenoid of suitable strength or other special set of magnetic elements at some point on a storage ring, it is possible to transform the spin orbit into a kind of Mobius strip such that, at a point on the storage ring opposite to the special magnets, the normal spin precession direction is longitudinal. The condition on the solenoid or set of magnets is that the spin rotates by exactly 180° about the beam direction in passing through the "Snake". When coupled to the usual precession about the vertical direction in the rest of the storage ring, the polarization direction will be in the plane of the orbit and be parallel to the beam diametrically opposite the Snake. The other curious feature of such a topology is that the spin advances by exactly π on successive orbital revolutions, not the usual $2\pi\nu$. This means that the effective spin tune is $\frac{1}{2}$ and the resonance condition Eq. (9) can, in general, be avoided at all energies. Thus, spin motion with a Siberian Snake is expected to be very stable.

In the simplest version of the Siberian Snake considered here, normal radiative polarization takes place perpendicular to the stable spin precession direction and it can only depolarize the beams. Thus, to use such a device, it will be necessary to inject already polarized beams. Somewhat more complicated arrangements should be able to avoid this effect if needed.³⁶

Currently, there is much theoretical activity in studying new approaches for providing longitudinally polarized beams³⁷ and polarized beams at high energies. Much of this work has been discussed at this Conference, and I shall not cover it here, except to refer to the talk of Derbenev.³⁶ There is still much work to be done in order to find practical arrangements for polarized beams that also allow the storage ring to function! Nevertheless, we can be reasonably optimistic about the prospect for such beams in future storage rings.

In conclusion, we have seen that beam polarization in high energy e^+e^- storage rings is a versatile tool for studying many phenomena. Probably the most significant result obtained to date is the very clear demonstration of the spin- $\frac{1}{2}$ quark character of the basic processes involved in hadron production by e^+e^- annihilation. The same behavior is seen in muon pair production, as expected from the theory of QED. The well understood process of spin precession makes beam polarization useful for energy calibration and other diagnostic functions. In future generations of storage rings and experiments using e^+e^- storage rings, there are many interesting measurements to be performed with polarized beams.

REFERENCES

1. A. A. Sokolov and I. M. Ternov, *Sov. Phys.-Dokl.* 8, 1203 (1964).
2. Y. S. Tsai, *Phys. Rev. D* 12, 3533 (1975).
3. See, for example: R. Budny, *Phys. Lett.* 45B, 340 (1973), and A. McDonald, *Nucl. Phys.* B75, 343 (1974).
4. I. M. Ternov, Yu. M. Loskutov, and L. I. Korovina, *Sov. Phys.-JETP* 14, 921 (1962).
5. V. N. Baier and V. M. Katkov, *Phys. Lett.* 24A, 327 (1967), and *Sov. Phys.-JETP* 25, 944 (1967).
6. V. N. Baier, *Sov. Phys.-Usp.* 14, 695 (1972), and *Proc. of the International School of Physics "Enrico Fermi," Varenna, 1969, Course XLVI (Academic Press, New York and London, 1972), pp. 1-49.*
7. J. D. Jackson, *Rev. Mod. Phys.* 48, 417 (1976).
8. V. Bargmann, L. Michel, and V. L. Telegdi, *Phys. Rev. Lett.* 2, 435 (1959).
9. Ya. S. Derbenev and A. M. Kondratenko, *Sov. Phys.-JETP* 35, 230 (1972).
10. Ya. S. Derbenev and A. M. Kondratenko, *Sov. Phys.-JETP* 37, 968 (1973).
11. Ya. S. Derbenev, A. M. Kondratenko, and A. N. Skrimskii, *Novosibirsk preprint #77-60 (1977).*
12. A. W. Chao, *SLAC technical note PEP-257/SPEAR-208 (1977).*

13. D. Potaux, Proc. of the 8th International Conference on High-Energy Accelerators, CERN, 1971, edited by M. H. Blewett (European Organization for Nuclear Research, Geneva, 1971), p. 127.
14. J. LeDuff *et al.*, Orsay technical report #4-73 (1973).
15. U. Camerini *et al.*, Phys. Rev. D 12, 1855 (1975).
16. W. T. Ford, A. K. Mann, and T. Y. Ling, SLAC report SLAC-158 (1972).
17. S. I. Serednyakov *et al.*, Sov. Phys.-JETP 44, 1063 (1976).
18. The members of the SPEAR polarization group are: G. E. Fischer, D. B. Gustavson, J. R. Johnson, J. J. Murray, T. J. Phillips, R. Prepost, R. F. Schwitters, C. K. Sinclair, and D. E. Wiser. A preliminary report of this work was presented to this conference by J. R. Johnson.
19. V. N. Baier and V. A. Khoze, Sov. J. Nucl. Phys. 9, 238 (1969).
20. S. I. Serednyakov *et al.*, Phys. Lett. 66B, 102 (1977).
21. R. S. Van Dyck, Jr., P. B. Schwinberg, and H. G. Dehmelt, Phys. Rev. Lett. 38, 310 (1977).
22. Ya. S. Derbenev *et al.*, Particle Accelerators 8, 115 (1978).
23. L. M. Barkov *et al.*, Novosibirsk preprint #77-74 (1977).
24. J. G. Learned, L. K. Resvanis, and C. M. Spencer, Phys. Rev. Lett. 35, 1688 (1975).
25. L. M. Kurdadze *et al.*, Novosibirsk preprint #75-66 (1975).
26. R. F. Schwitters *et al.*, Phys. Rev. Lett. 35, 1320 (1975).
27. G. Hanson *et al.*, Phys. Rev. Lett. 35, 1609 (1975).
28. A. W. Chao, SLAC technical note PEP-263 (1978).
29. B. Richter, Nucl. Instrum. Methods 136, 47 (1976).
30. D. Möhl and B. W. Montague, Nucl. Instrum. Methods 137, 423 (1976).
31. Ya. S. Derbenev, A. M. Kondratenko, and A. N. Skrinsky, Novosibirsk preprint #76-62 (1976).
32. See, for example: J. Ellis and M. K. Gaillard, Physics With Very High Energy e^+e^- Colliding Beams, CERN report 76-18 (1976), p. 39.
33. N. Christ, F.J.M. Farley, and H. G. Hereward, Nucl. Instrum. Methods 115, 227 (1974).
34. R. Schwitters and B. Richter, SLAC technical note PEP-87/SPEAR-175 (1974).
35. Ya. S. Derbenev and A. M. Kondratenko, Novosibirsk preprint #76-84 (1976).
36. Ya. S. Derbenev, invited talk at this Conference.
37. Ya. S. Derbenev, A. M. Kondratenko, and E. L. Saldin, Novosibirsk preprint #78-61 (1978).